

Stratospheric control of upward wave flux near the tropopause

R. K. Scott and L. M. Polvani

Department of Applied Physics and Applied Mathematics, Columbia University, New York, USA

Received 13 June 2003; revised 29 August 2003; accepted 5 December 2003; published 30 January 2004.

[1] Using an idealized, global primitive equation model of the stratosphere-troposphere system in which all tropospheric variability is suppressed, we demonstrate the existence of internal modes of stratospheric variability. The variability in our model is similar to that observed in the winter stratosphere, consisting of sudden-warming like, wave-driven decelerations of the polar vortex followed by a more gradual re-establishment of the vortex by the radiative forcing. Using a common index of the strength of the stratospheric vortex, we find patterns of downward propagation resembling those found in recent observations. In addition, our model exhibits considerable variability in the upward flux of wave activity into the stratosphere; this variability strongly anti-correlates with the index of the mid-upper stratospheric vortex, again in agreement with recent observations. *INDEX TERMS*: 3334 Meteorology and Atmospheric Dynamics: Middle atmosphere dynamics (0341, 0342); 3362 Meteorology and Atmospheric Dynamics: Stratosphere/troposphere interactions; 3367 Meteorology and Atmospheric Dynamics: Theoretical modeling. *Citation*: Scott, R. K., and L. M. Polvani (2004), Stratospheric control of upward wave flux near the tropopause, *Geophys. Res. Lett.*, 31, L02115, doi:10.1029/2003GL017965.

1. Introduction

[2] There has been increasing interest in recent years in the possibility that events or trends in the stratosphere may have an influence on, or provide an early indicator of, tropospheric patterns of variability, on both sub-seasonal and climatological time-scales. In particular, on time scales of several weeks, there is evidence that extreme events in the stratosphere precede definite preferred patterns in the troposphere and surface weather [Baldwin and Dunkerton, 2001; Thompson *et al.*, 2002]. The source of stratospheric variability, however, is yet to be fully determined.

[3] In a recent study, Polvani and Waugh [2004] have shown that the Northern Annular Mode (NAM) index of stratospheric variability at 10 hPa (used by Baldwin and Dunkerton [2001] to define extreme events) is strongly correlated with the time integrated flux of wave activity entering the stratosphere prior to a particular day. From this, one might be tempted to conclude that the stratosphere is simply a mediator of tropospheric variability, passively reacting to forcing from below.

[4] On the other hand, there is evidence from severely truncated numerical models that the stratosphere may also possess its own, internal modes of variability [Holton and Mass, 1976; Yoden, 1987, 1988; Scott and Haynes, 2000]. An open question is whether models with more adequate

horizontal and vertical resolutions would also exhibit internal modes of variability. A recent GCM study suggests that this may be the case [e.g., Christiansen, 1999], but the underlying dynamics remains unclear.

[5] In this letter we show that simple yet realistically truncated models possess strong modes of internal variability. More importantly, we also show that this variability arises through the ability of the stratosphere itself to control the amount of wave activity entering it from the troposphere below. Thus, while the source of wave forcing resides in the troposphere, the state of the stratosphere nevertheless plays a crucial role in determining the onset of extreme stratospheric events, and consequently has an influence on the preferred patterns of the ensuing tropospheric circulation.

2. Method

[6] Our model solves the dry, primitive equations on the sphere, the vertical domain extending from the ground to approximately 80 km. We compute with 40 vertical levels and a “T42” horizontal resolution (equivalent to a grid spacing of approximately 2.8 degrees).

[7] The stratosphere is thermally forced using Newtonian relaxation to an equilibrium profile with cooler temperatures over the winter pole; this produces a polar vortex. To prevent the generation of unrealistically large westerly winds in the upper stratosphere and mesosphere, a Rayleigh drag is included above 0.5 hPa. This also acts as a sponge to prevent spurious wave reflection from the upper boundary.

[8] In the troposphere, all variability is suppressed by a combination of thermal relaxation and Rayleigh drag. The thermal equilibrium to which the model troposphere is relaxed is constant in latitude, and therefore baroclinically stable. Rayleigh drag on the mean flow ensures weak tropospheric westerlies on which the waves can propagate upward into the stratosphere. Stationary planetary waves are forced in the lower troposphere with a time-independent wave-1 heating.

[9] For complete reproducibility, full details regarding the model and the forcing functions are included in the appendix. We emphasize that *all* forcings, in the troposphere as well as the stratosphere, are time-independent.

3. Results

[10] Figure 1 shows the zonally averaged zonal velocity at 60°N, near the latitude of the polar vortex jet maximum, as a function of height and time from a typical 4000 day perpetual January integration. The forcing values, which are given in the appendix, have been chosen to give wind speeds representative of the NH winter stratosphere.

[11] For the chosen parameter values, the polar vortex exhibits a clear mode of internal variability on a timescale of

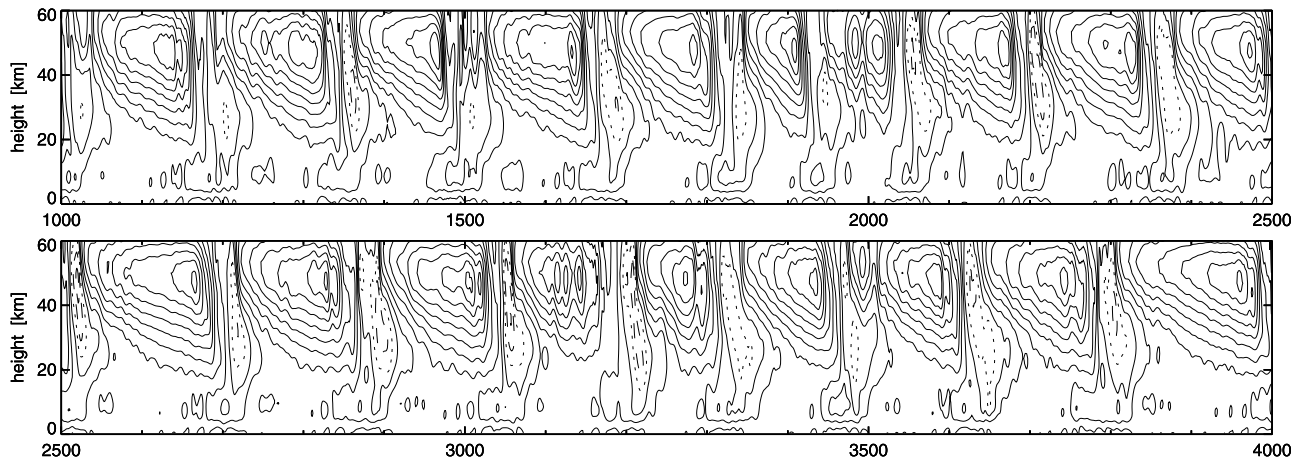


Figure 1. Zonal mean zonal velocity at 60°N as a function of height (in km) and time (in days). Numerical resolution is T42, with 40 vertical levels. The topspheric wave forcing amplitude $A = 2 \times 10^{-4} \text{ K s}^{-1}$, and the radiative equilibrium vortex strength $\gamma = 2$. The contour interval is 10 m s^{-1} , with positive, negative, and zero values shown solid, dashed, and dotted, respectively.

approximately 160 days. This variability is characterized by a sudden deceleration of the polar vortex, similar in character to a major stratospheric sudden warming, followed by a gradual reacceleration of the vortex under radiative relaxation. We emphasize that there is no time dependence in any of the model forcings: both the wave forcing and the radiative relaxation are time-independent. Thus the variability of the stratosphere arises *solely* as a result of the internal, wave-mean flow dynamics of the atmospheric circulation.

[12] In addition, we have determined that the above behaviour is robust, with qualitatively similar variability exhibited over a wide range of parameter values and numerical resolution. Full details of the parameter and resolution dependence, as well as a comparison with modes of variability obtained by previous authors, will be reported in a separate study.

[13] A closer look at Figure 1 shows that the sudden warming begins in the upper stratosphere and is followed by deceleration of the mean flow at progressively lower levels, giving rise to a downward propagating region of deceleration similar to that originally reported in *Kodera et al.* [1990]. In our model, the downward propagation is unable to penetrate into the troposphere because of the strong constraint on the mean flow there. However, there is downward propagation over several scale heights, spanning the region from around 50 km down to around 20 km.

[14] Notwithstanding the quiescent nature of our model troposphere and the idealized nature of our model, we compare the downward propagating sudden-warming type events described above with the extreme weak vortex events described in *Baldwin and Dunkerton* [2001]. Following Baldwin and Dunkerton we construct an annular mode index based on a singular value decomposition of the daily, unweighted geopotential height field at each model level, and define a weak vortex event as the day on which the index at 1 hPa exceeds a value of 2.0. A similar pattern was obtained using the value of the index at 10 hPa.

[15] Figure 2 shows the NAM index as a function of height and time-lag from the event day from composites of 21 weak vortex events, (compare *Baldwin and Dunkerton*, [2001], Figure 2a). Note that only weak vortex events are

dynamically significant in our model, strong vortex states corresponding simply to the intervening periods in which the vortex strengthens under radiative effects. Such an asymmetry was also found by *Baldwin and Dunkerton* [2001] in the observed stratospheric NAM.

[16] To demonstrate that the stratospheric variability in our model arises from the (steady) tropospheric wave forcing rather than from some local upper stratospheric instability, we follow *Polvani and Waugh* [2004] and compare the upward wave flux entering the stratosphere, integrated over a time interval T preceding a given day, with the value of the stratospheric NAM index on that day. Figure 3 shows the NAM index at 10 and 1 hPa together with the vertical component of the Eliassen-Palm (EP) flux at 200 hPa, averaged over the Northern Hemisphere, that is, $\int_0^2 F^{(z)} \cos \phi \, d\phi$ where $\mathbf{F} = \{F^{(\phi)}, F^{(z)}\}$ is the EP flux as defined by *Andrews et al.* [1987, Equation 3.5.3]. The strong anti-correlation between the two quantities, which maximizes for an integration time interval of $T = 28$ days with a value of -0.94 for the 10 hPa NAM, indicates that the upper stratospheric variability is indeed related to the variability in the upward propagation of wave flux from the troposphere. Strong anti-correlations were found for a wide

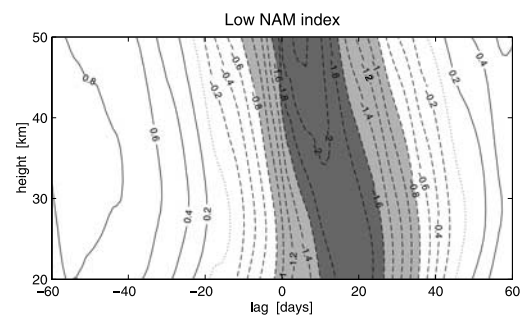


Figure 2. NAM index for a composite of 21 weak vortex events, based on the value of the NAM at 1 hPa, as a function of height and time lag in days from the onset of the event. Light and dark shading corresponds to values less than -0.8 and -1.6 , respectively.

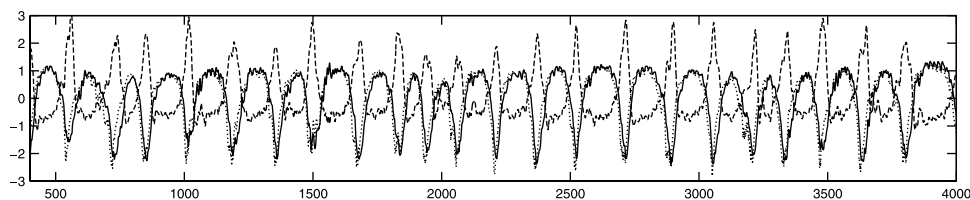


Figure 3. Stratospheric NAM indices, derived from an SVD of geopotential height at 10 hPa (solid) and at 1 hPa (dotted) together with the upward wave flux into the stratosphere (dashed), defined as the latitudinally averaged vertical component of EP flux through 200 hPa, integrated in time over 28 days preceding a given day. All quantities are normalized to have zero mean and unit variance.

range of T , at both 10 hPa and 1 hPa. *Polvani and Waugh* [2004] found similarly strong anti-correlations in 40 years of NCEP reanalyses. The important point to note here, however, is that the wave flux out of the forcing region (below 200 hPa) is highly variable despite the fact that the wave forcing itself is entirely time-independent.

[17] Because of this, and the fact that our model troposphere is nearly quiescent, the amount of wave activity propagating into the upper stratosphere must be determined solely by the state of the stratosphere itself. Thus, during and prior to a weak vortex event, conditions are such that upward wave propagation into the upper stratosphere is enhanced. In contrast, when the vortex is strong conditions are such that upward wave propagation is suppressed.

[18] Finally, we show that the downward propagation of the region of vortex deceleration is primarily a result of wave-mean flow interaction, in agreement with the results of *Christiansen* [1999]. In Figure 4a we plot the latitudinally averaged EP flux divergence, $\int_0^z \nabla \cdot \mathbf{F} \cos \phi d\phi$, as a function of height and time, for a subinterval of the model integration containing two typical weak vortex events. This quantity represents the total momentum forcing of the mean flow by wave dissipation. As seen in the figure, a region of wave flux convergence (easterly momentum forcing) begins in the upper stratosphere and moves downward as the structure of the mean flow changes in response to the wave dissipation, similar to *Matsuno's* [1971] model of stratospheric sudden warmings. A careful comparison of this figure with the zonal mean zonal velocity field at 60°N indicates that the timing of the wave dissipation matches that of the strong mean flow deceleration events. Similar dynamics were found by *Plumb and Semeniuk* [2003] in a stratosphere only model; however, the forcing at the lower boundary in that model was time-dependent.

[19] To relate the stratospheric wave dissipation shown in Figure 4a to the wave flux entering the stratosphere, we show in Figure 4b, the latitudinally averaged vertical EP flux into the stratosphere through 200 hPa over the same subinterval of the integration. Wave fluxes into the stratosphere continue to increase beyond the onset of the deceleration in the upper stratosphere, right up until the reversal of the mean winds in the lower stratosphere. Indeed, such an increase is necessary to sustain the continued downward propagation of the wind reversal because of the larger mass of the lower stratosphere. When the easterlies penetrate to sufficiently low levels, the upward propagation of waves is finally shut off, and the vertical EP flux drops suddenly to near zero. It then remains small for some time allowing the upper stratospheric winds to recover under the effect of the radiative relaxation. Note that *Polvani and Waugh* [2004]

found a similar peak in the upward wave flux into the stratosphere during observed weak vortex events, as well as the subsequent sudden decrease to near zero values following the reversal to easterly winds in the lower stratosphere.

4. Conclusions

[20] Using an idealized stratosphere-troposphere model in which the troposphere is quiescent, we have demonstrated that the stratosphere is able to generate its own internal variability. This corroborates the results of earlier, highly truncated models. The variability in our model is characterized by rapid deceleration of the mean flow, caused by strong wave-mean flow interaction and resembling a stratospheric sudden warming, followed by a more gradual recovery under

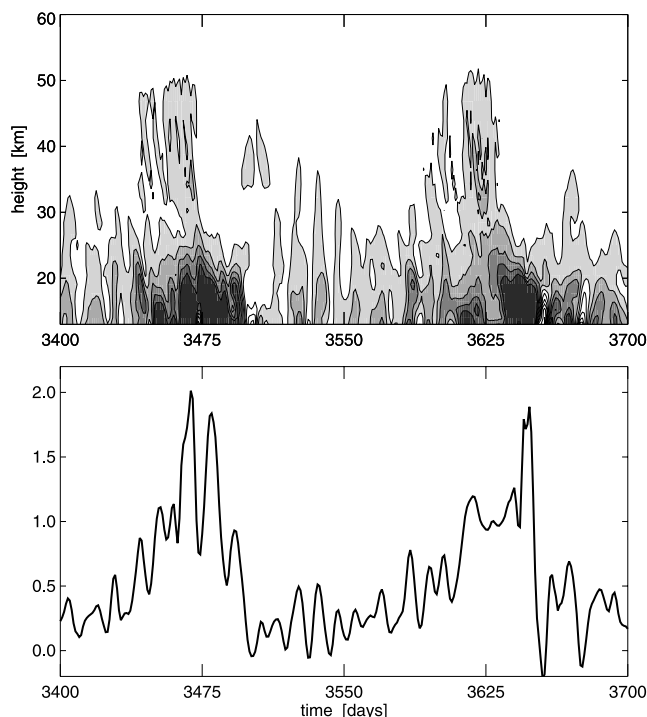


Figure 4. (a) latitudinally averaged EP flux divergence, as a function of height and time for a representative subinterval of the model integration; (b) latitudinally averaged upward EP flux through 200 hPa as a function of time for the same subinterval. The contour interval in (a) is $10^{14} \text{ kg m s}^{-2}$, with negative values (convergence) shaded and darker tones corresponding to larger negative values. Units in (b) are $10^{19} \text{ kg m}^2 \text{ s}^{-2}$.

radiative relaxation. A height, time-lag plot of the stratospheric NAM index based on a composite of weak vortex events resembles closely the structure of that found previously in observations, including the characteristic downward phase propagation.

[21] Although all forcing in our model is time-independent, large variability is found in the upward wave flux entering the stratosphere at 200 hPa. This variability anticorrelates strongly with the NAM at 10 hPa and above. The downward descent of the deceleration phase of the event relies on the continued increase of upward wave flux into the stratosphere, right up until wind reversal in the lower stratosphere, and long after the initiation of the sudden warming event in the upper stratosphere. Since the tropospheric forcing is time-independent, the continued increase in upward wave flux must be governed by the internal dynamics of the sudden warming process itself, rather than by details of the forcing.

[22] As a further test of the robustness of this result, we have repeated the calculations presented above using a stratosphere-only model, in which the vertical domain is restricted to 200 hPa and above, and in which the lower boundary condition includes a time-independent wave-1 forcing on the geopotential height field. Similar internal variability of the circulation and of the upward wave flux through the lower boundary was found. A more complete discussion of the results from both of these model configurations, stratosphere/troposphere and stratosphere only, will be reported in a separate study.

[23] Our results may have implications for our understanding of the dynamics accompanying major sudden warming events and of the influence of the stratosphere on the tropospheric variability. Although our study suggests that stratospheric variability may exist in the absence of tropospheric variability, the latter is likely to play some role. What this role is remains to be determined.

Appendix

[24] We use a semi-spectral, pressure coordinate model to solve the primitive equations in a spherical domain. The model is the BOB (Built on Beowulf) dynamical core developed jointly at NCAR and Columbia University, and numerical details, implementation and availability are documented fully in Rivier *et al.* [2001] and Scott *et al.* [2003].

[25] The horizontal resolution used for the results presented is T42. There are 41 “half-levels” in the vertical between 1000 hPa and 0 hPa located at pressures given by the values of $(i/N)^5 \times 10^3$ hPa for integer values $i = 0, 5, 6, 7, \dots, N$ with $N = 44$. The 40 “full-levels” are then located at the mid points of the half-levels.

[26] The radiative equilibrium temperature corresponds to an isothermal atmosphere plus a cooling over the winter pole: $T_e = (1 - w(\phi))T_0 + w(\phi)T_{PV}(p)$ where $w(\phi) = (1 - \tanh((\phi - \phi_0)/\delta\phi))/2$ and $T_{PV}(p) = T_0 \min(1, (p/p_T)^{-\gamma/g})$, with $T_0 = 240$ K, $\phi_0 = 50^\circ$, $\delta\phi = 20$, and $p_T = 200$ hPa. In the integration presented, $\gamma = 2$. The rate at which temperatures are relaxed to T_e is as in Holton [1976].

[27] Waves are forced in the model using a wavenumber-1, time-independent tropospheric heat source of the form $Q = A_0 G(\phi) Z(p) \cos\theta$, where θ is longitude, $G(\phi > \phi_1) = \sin^2[(\phi - \phi_1)/(\frac{\pi}{2} - \phi_1)]$, $G(\phi \leq \phi_1) = 0$, with $\phi_1 = 30^\circ$, and where $Z(p > p_T) = \cos^2(\frac{\pi}{2} \frac{z}{z_T})$, $Z(p \leq p_T) = 0$, with $z = -H \log \frac{p}{p_s}$, $H = 7000$ m, $p_s = 1000$ hPa, and $z_T = z(p_T)$. In the integration presented the amplitude $A_0 = 2 \times 10^{-4}$ K s⁻¹.

[28] To allow the forced waves to propagate vertically, weak westerly flow is forced in the troposphere by relaxing the mean flow to a barotropic profile of the form $u_T(\phi) = U \sin^2(2\phi)$, with $U = 30$ m s⁻¹. The relaxation rate is $k_T Z(p)$, with $k_T = 1/\text{day}$. A tropospheric sponge, damping at the same rate, is included on wavenumbers 2 and higher.

[29] A sponge layer is included above $p_{sp} = 0.5$ hPa, damping both the waves and the mean flow at a rate $k_{sp} \max(0, ((p_{sp} - p)/p_{sp})^2)$, with $k_{sp} = 2/\text{day}$.

[30] Finally, numerical diffusion is included using a scale-selective ∇^8 hyperdiffusion, with a diffusion time scale of half a day at the smallest scales.

[31] **Acknowledgments.** The authors wish to thank Darryn Waugh and Mark Baldwin for helpful discussions and comments. This work was supported by the US National Science Foundation and by the David and Lucile Packard Foundation.

References

- Andrews, D. G., J. R. Holton, and C. B. Leovy (1987), *Middle Atmosphere Dynamics*, Academic Press.
- Baldwin, M. P., and T. J. Dunkerton (2001), Stratospheric harbingers of anomalous weather regimes, *Science*, *294*, 581–584.
- Christiansen, B. (1999), Stratospheric vacillations in a general circulation model, *J. Atmos. Sci.*, *56*, 1858–1872.
- Holton, J. R. (1976), A semi-spectral numerical model for wave, mean-flow interactions in the stratosphere: Application to sudden stratospheric warmings, *J. Atmos. Sci.*, *33*, 1639–1649.
- Holton, J. R., and C. Mass (1976), Stratospheric vacillation cycles, *J. Atmos. Sci.*, *33*, 2218–2225.
- Kodera, K., M. R. Yamazaki, M. Chiba, and K. Shibata (1990), Downward propagation of upper stratospheric mean zonal wind perturbation to the troposphere, *Geophys. Res. Lett.*, *17*(9), 1263–1266.
- Matsuno, T. (1971), A dynamical model of the stratospheric sudden warming, *J. Atmos. Sci.*, *28*, 1479–1494.
- Plumb, R. A., and K. Semeniuk (2003), Downward migration of extratropical zonal wind anomalies, *J. Geophys. Res.*, *108*(D7), 4223, doi:10.1029/2002JD002773.
- Polvani, L. M., and D. W. Waugh (2004), Upwelling wave activity flux as a precursor to extreme stratospheric events and subsequent anomalous surface weather regimes, *J. Clim.*, in press.
- Rivier, L., R. Loft, and L. M. Polvani (2001), An efficient spectral dynamical core for distributed memory computers, *Mon. Weather Rev.*, *130*, 1384–1390.
- Scott, R. K., and P. H. Haynes (2000), Internal vacillations in stratosphere-only models, *J. Atmos. Sci.*, *57*, 2333–2350.
- Scott, R. K., L. Rivier, R. Loft, and L. M. Polvani (2003), BOB: Model implementation and users guide, *NCAR Technical Note*.
- Thompson, D. W. J., M. P. Baldwin, and J. M. Wallace (2002), Stratospheric Connection to Northern Hemisphere Wintertime Weather: Implications for Prediction, *J. Clim.*, *15*, 1421–1428.
- Yoden, S. (1987), Dynamical aspects of stratospheric vacillations in a highly truncated model, *J. Atmos. Sci.*, *44*, 3683–3695.
- Yoden, S. (1988), Bifurcation properties of a stratospheric vacillation model, *J. Atmos. Sci.*, *44*, 1723–1733.

R. K. Scott, Mathematical Institute, University of St Andrews, St Andrews, KV16 9SS, Scotland. (richard@mcs.st-and.ac.uk)

L. M. Polvani, Department of Applied Physics and Applied Mathematics, Columbia University, New York, USA. (lmp@columbia.edu)